UNDERSTANDING THE INFLUENCE OF MANUFACTURING DEFECTS ON THE TENSILE BEHAVIOR OF SIC/SIC FILAMENT WOUND TUBES FROM A UNIDIRECTIONAL COMPOSITE MODEL

Claire Morel, Emmanuel Baranger, Jacques Lamon, James Braun, Christophe Lorrette

UNDERSTANDING THE INFLUENCE OF MANUFACTURING DEFECTS ON THE TENSILE BEHAVIOR OF SIC/SIC FILAMENT WOUND TUBES FROM A UNIDIRECTIONAL COMPOSITE MODEL

Claire, Morel[a,b], Christophe, Lorrette[a], James, Braun[a], Jacques, Lamon[b], Emmanuel, Baranger[b]

[a]: Université Paris-Saclay, CEA, Service de Recherches Métallurgiques Appliquées, 91191, Gif-sur-Yvette, France – claire.morel@cea.fr ;
[b]: Université Paris-Saclay, Centrale Supélec, ENS Paris-Saclay, CNRS, LMPS - Laboratoire de Mécanique Paris-Saclay, 91190, Gif-sur-Yvette, France.

Abstract: *SiC/SiC ceramic matrix composites are promising cladding candidates to improve the accident tolerance of the fuel in pressurized water reactors. Indeed, their excellent mechanical properties at high temperatures (above 1200°C) would give them additional margins to face a loss of coolant. In this work, the mechanical behavior of a filament wound tube under cyclic tensile stress is performed in order to investigate the impact of two types of manufacturing defects on the mechanical behavior. The defects studied correspond to local modifications of the composite microstructure. For both classes of defects, the same methodology is used, consisting in performing mechanical cyclic tensile tests in the tube axis direction with post-analysis to assess fine parameters. The results allow characterizing the elastic behavior, as well as, the behavior during matrix microcracking through the consideration of unload-reload cycles. Microstructiral analyses are performed to establish the mechanical properties/microstructures relationship.*

Keywords: mechanical behavior; manufacturing defects; SiC/SiC; tubes

1. Introduction

Ceramic matrix composites (CMC) are attractive materials for high-temperature applications, due to their stability up to 1600°C [1]. Therefore, they are studied with a view to application in many high value-added fields. For example, these materials, and more specially the SiC/SiC composites are prime candidates for fuel cladding in pressurized water reactors, because of their high temperature resistance and their stability under irradiation when materials are pure and well-crystallized [2]. Using SiC/SiC composites could increase reactor safety, especially for E-ATF (Enhanced Accident Tolerant Fuels) applications, aiming to improve fuel cladding properties in the event of a loss-of-coolant accident (LOCA) [3]. In fact, unlike zirconium-based fuel cladding, SiC/SiC composites can maintain their geometry and integrity in extreme situations (beyond 1200°C in oxidizing steam environment). They show a strongly reduced oxidation compared to zirconium-based fuel cladding under such accident conditions.

The mechanical behavior of SiC/SiC CMC has been studied widely in the literature either experimentally or by modeling. Unidirectional composite have been investigated with the shear lag model [4, 5] and 2D plate architectures have already been characterized [6]. Attention will then be focused on tubular architecture in this work. Less data are found in the literature in this field because few applications use this geometry, outside nuclear and some aeronautical ones [7].

In this paper, two batches of tubular test specimens representative with dimensions of fuel cladding tubes were studied [8]. Each batch presented a local modification of the morphology,

  doi:10.5075/epfl-298799_978-2-9701614-0-0

the first one consisting in variation of core chemical composition while the second one in surface defects. The objective of this paper is to describe the damage phenomena of various SiC/SiC tubes with various microstructure characteristics by relying on a damage models for unidirectional composites. In a first part, the material is described, as well as the experimental protocol of the tensile tests. In a second part, the analysis of the mechanical behavior is carried out.

2. Description of material and tensile tests

2.1 Manufacturing process of SiC/SiC tubes

The tubes were made of three components: silicon carbide (SiC) fibers, SiC matrix and pyrocarbon (PyC) fiber/matrix interphase. The fibrous preform was made of 3rd generation Hi-Nicalon type S fibers. Two reinforcement layers were produced by filament winding with an angle of +/-45° along the tube axis, using cylindrical tooling to ensure tubular geometry and good surface finish. The PyC and SiC were deposited by Chemical Vapor Infiltration (CVI). In a first step, pyrocarbon interphase with a thickness between 50 and 100 nm was deposited on fibers, in order to optimize fiber/matrix coupling and to promote deflection of the matrix cracks. Then, a first layer of matrix was deposited to consolidate the structure and allow the mandrel removal by chemical attack [9]. Two successive infiltration cycles finalized the tubes densification. Finally, external and internal finishing surface treatment steps were possible. In this study, only the influence on grinding will be conducted for this step. The dimensions of the tubes were given in Table 1 and 2; the average cross section area of tubes was 17mm².

2.2 Manufacturing defects

The two types of local morphology changes investigated are referred to as defects in the following. The first defect type refers to a change in core composition, while the second results from grinding step. The tubes were assumed to be composed of two parts: the plies, consisting of matrix, fibers and porosity and the outer surfaces of the tube, called seal coat, composed of matrix only.

Table 1 details the composition of the two grades of tubes of batch 1. Within the plies, porosity was lower in grade 1-B than in grade 1-A. Indeed, in grade 1-B, the matrix within the plies, deposited during the first CVI step, was not pure and contained silicon, unlike grade 1-A which contained only SiC. This can been explained by the conditions during the CVI cycles that differed from the nominal conditions.

Batch 2 was dedicated to the investigation of the influence of surface defects. For this purpose, different amounts of seal coat were removed by grinding from the inner and the outer surfaces. 2-RR grade denotes reference as-manufactured tubes. The following grades (2-OI, 2-O+I and 2-O+I+) refer to all outer and inner grinded tubes, respectively noted O and I. Thickness of remaining seal coat and tube dimensions for the different grades are given in Table 2.. The seal coat had been completely removed during the grinding operation for those tubes labelled with a "+". On those surfaces, plies are directly uncovered and some fibers have been damaged by the grinding operation. On the other tubes, the seal coat was still present on the surface of fiber preform and it was expected to smooth the external surfaces.

Table 1: Characteristics of the microstructures of the two grades of the batch 1.

Batch 1		1-A	1-B
Tube	Outer diameter	9.59 mm	9.50 mm
	Inner diameter	8.31 mm	8.22 mm
External layers	Outer thickness	65 µm	30 µm
	Inner thickness	53 µm	100 µm
Plies	Fiber fraction	40 %	34 %
	Porosity	7.7 %	5.3 %
	Matrix fraction	52.3 %	60.7 %

Table 2: Characteristics of the microstructures of the two grades of the batch 2.

Batch n°2		2-RR	2-OI	2-O+I	2-O+I+
Tube	Outer diameter	9.68 mm	9.53 mm	9.28 mm	9.31 mm
	Inner diameter	8.31 mm	8.32 mm	8.28 mm	8.43 mm
External layers	Outer thickness	84 µm	75 µm	0 µm	0 µm
	Inner thickness	58 µm	61 µm	58 µm	0 µm
Plies	Fiber fraction	37 %			
	Porosity	8.5 %			
	Matrix fraction	54.5 %			

2.3 Cyclic tensile test protocol

Figure 1. Set-up of cyclic tensile tests.

Tensile tests were performed on tubes from both batches. Load was applied parallel to tube axis leading to a local multi-axial loading of each ply. The test procedure is described in ISO 20323 standard [10]. The specimens were 65 mm and 70 mm long for batch 1 and 2, respectively. The tubes were glued in a mandrel with epoxy adhesive. The tube and gripping clamp assembly was

installed on the testing device. The upper part was screwed on it, while the lower part was directly glued to a grip itself screwed to the lower part of the tensile machine (see Fig. 1). This method guarantees tube alignment with respect to the loading direction [10]. The force was measured with a 25 kN load cell (HBM U10M). The strain was measured thanks to longitudinal extensometers with 25 mm (INSTRON 2620-603) and 30 mm (MFA1) gauges length for the batch 1 and 2, respectively. Loading rate was 0.05 mm/min.

Cyclic as well as monotonic loading mode was applied on batch 1. A maximum of 4 cycles were performed, with a single one is in the elastic domain, with a minimum stress of - 50 MPa at each cycle. The number of cycles and the level of damage were sufficiently low to avoid fatigue phenomena [8]. An example of the stress-strain curve for a cyclic test is shown in Figure 2.

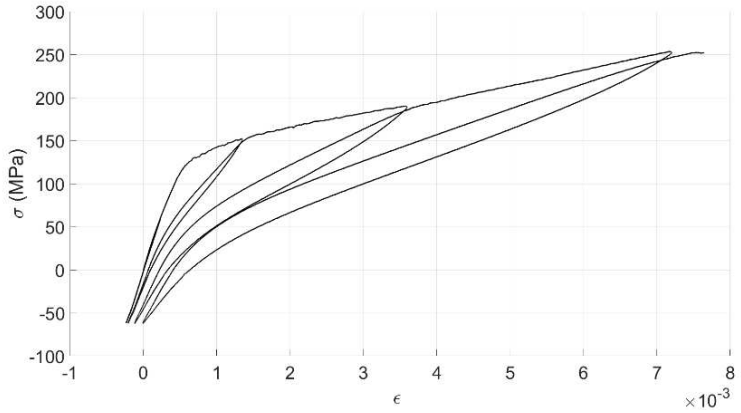

Figure 2. Mechanical behavior curve for grade 1-A.

3. Mechanical behavior

3.1 Elastic behavior

The Young's moduli are given in Figure 3. It can be noticed that the 1-B grade presents a softer behavior than 1-A (resp. 213 GPa on average against 271 GPa). This was attributed to the presence of silicon in the matrix core. Indeed, the elastic modulus of silicon is around 150 GPa against 416 GPa for the CVI-SiC (β-SiC) matrix [11]. For the 2nd batch, when the seal coat is removed, the elastic modulus of tube decreases. The seal coat matrix is stiffer than the core composed of fiber, matrix and porosity.

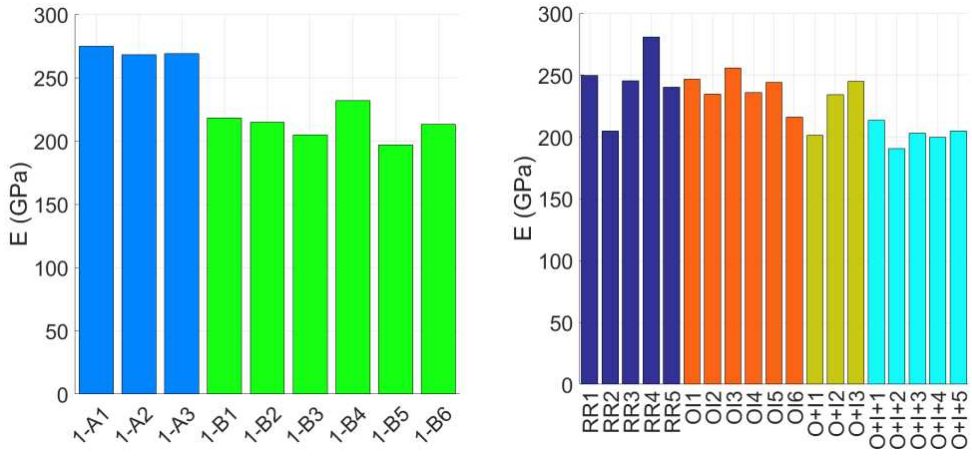

Figure 3. Elastic modulus for batch 1 (left) and batch 2 (right).

In parallel, an analytical model was developed to simulate tube elastic behavior as a function of the composition. This model is based on the equations of the continuous media mechanics (hypothesis of small perturbations and equilibrium). For each layer of tube, a behavior law was determined. For the seal coat, an isotropic behavior was assumed [11]. For the core layers, the behavior was determined in three steps. At first, only the isotropic matrix was considered then pores were added by assimilating them to blunt cracks [12] and finally, the behavior of the fibers fiber was added only in the fiber axis.

The experimental and analytical analysis of elastic behavior enabled to assess the role of the external layers of matrix. The latter stiffen the composite owing to their composition (i.e. layers with only matrix, without porosity) and increase the isotropy of tube structure. When the thickness of tubes is reduced, the external layer tend to play the same role as the internal layer of matrix, for the same thickness. On the other hand, the study of the onset of matrix cracking, not detailed in this paper, shows that the external seal coat layers crack first, especially the outer matrix layer. The outer SiC grains present a more fragile behavior because of their specific microstructure consisting in large columnar arrangement.

3.2 Damage behavior

The tube damage behavior was then studied. In the case of unidirectional CMC, the first cracks appear in the matrix. These cracks are then deflected at the fiber/matrix interface (Figure 4). Therefore, a load transfer occurred from the matrix onto the fibers. In addition, around the cracked areas, debonding between the fiber and the matrix appeared. Slip between the fiber and the matrix took place, characterized by the shear stressτ. Different quantities characterize the damage in the composite, particularly in cyclic tests [4]. In this paper, a focus on two quantities highlighting the impact of the two defects was studied.

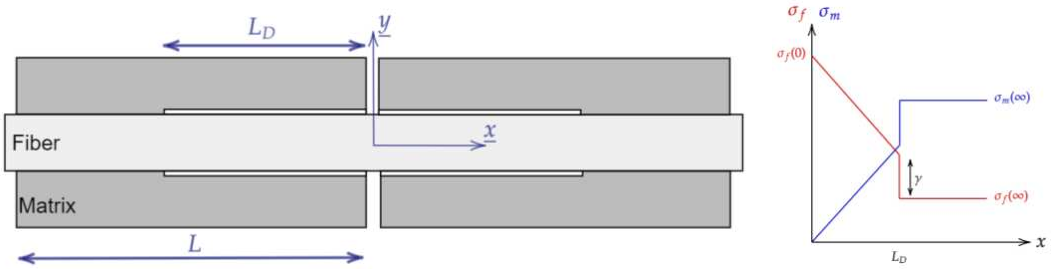

Figure 4. Shear lag model.

The cycle width at half-maximum characterizes the slippage in the composite [4] (see Fig. 2). Indeed, during a cycle, no new crack occurs; the hysteresis induced by the energy loss was only due to slippage. In unidirectional composites, slippage is located at the fiber/matrix interface. However, slippage in the tubes can occur between fiber and matrix in the core preform or between the plies. Figure 4 shows the evolution of the slippage during the cycles for the two batches as a function of the strain at the beginning of the cycle.

On the 2nd batch, no difference between the grades was observed. The external layers of the matrix had no impact. Slippage was essentially located in the fibrous preform, at the fiber/matrix interface or between the plies. Therefore, the shear lag model can be applied.

On the 1st batch, a difference was observed. The slippage is more important on grade 1-A. In a first approximation, it was assumed that the preform behaves like a unidirectional composite. Thus, the effect of the fiber orientation and the shear stress associated with this orientation were neglected. According to the shear lag model [5,6], the stresses in the matrix at a given level of a crack were defined by equation Eq. (1).

$$\frac{2\tau L_D}{R_f} = \sigma_m(\infty) - \gamma + \sigma_m^T \quad (1)$$

with R_f the fiber radius, γ the equivalent stress of the energy jump at the level of matrix break, σ_m^T the thermal residual stress and $\sigma_m(\infty)$ the stress in the matrix away from the crack. Debonding length was defined by Eq. (2). Thus, as the elastic matrix modulus E_m in the matrix decreased, debonding length decreased. The fiber/matrix slippage occurred over a shorter area, leading to thinner cycles width, which confirmed the experimental observations (Figure 5).

$$L_D = \frac{R_f}{2\tau}(E_m\epsilon(\infty) - \gamma + \sigma_m^T) \quad (2)$$

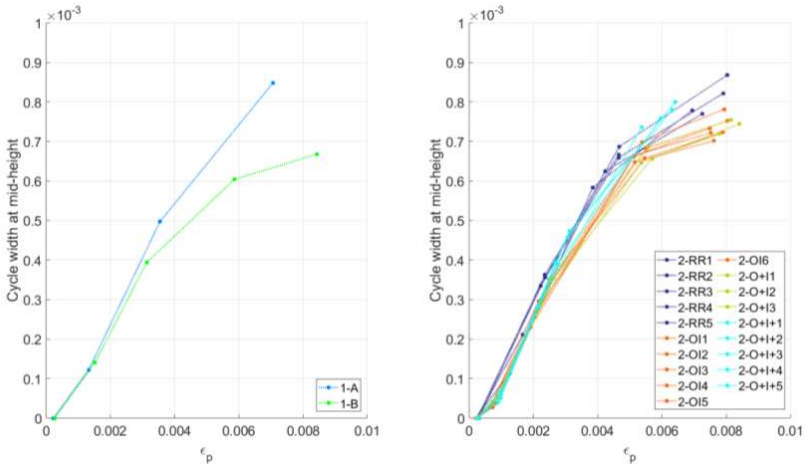

Figure 5. Cyclic width at mid-height in function of the strain for batch n°1 (left) and batch n°2 (right).

The second characteristic quantity considered is the evolution of the tangent modulus at the beginning of discharge $1/E^*$. Figure 5 shows its evolution for the two batches as a function of the strain at the beginning of the cycle. This quantity characterizes the damage evolution within the composite.

First, the impact of matrix seal coat on the damage was studied on the 2nd batch. By analyzing the micrographs in the final state and studying the properties at breakage of the different components, it was evidenced that the external layers of the tube were cracked. However, the presence of matrix seal coat seemed to have no impact on the tube damage. In order to justify this experimental observation, a simplified model was considered. It was composed of two layers: the first one ($\cdot_c$), in the core, and two external layers ($\cdot_e$). In the following, the cross-sectional area, the damage and the elastic modulus of each layer will be noted as $S_\cdot$, $d_\cdot$ and $E_\cdot^0$ respectively. The damage behavior of this two-layer material as given in Eq. (3), allowed the strength N and the strain ϵ to be related. The equivalent damage of the two layers $\overline{d}$, was deduced as Eq. (4).

$$N = [S_e E_e^0(1 - d_e) + S_c E_c^0(1 - d_c)]\epsilon \quad (3)$$

$$\overline{d} = 1 - \frac{S_e E_e^0 (1-d_e) + S_c E_c^0 (1-d_c)}{S_e E_e^0 + S_c E_c^0} \quad (4)$$

$$\alpha = S_e E_e^0 / S_c E_c^0 \quad (5)$$

Moreover, by considering the section ratios and by performing a Taylor expansion of α defined by Eq. (5), Eq. (6) is obtained. Therefore, the core layer was well predominant in the damageable behavior of the composite.

$$\overline{d} \approx d_c + \alpha(d_e - d_c) \quad (6)$$

On the 1st batch, a slight difference was noticed between the two grades, which is due to the differences measured in the elastic domain (≈ 20%). The core composition change modified in a similar way the tangent modulus E^* but did not influence the damage evolution. The measurement of the tangent modulus $E^*$was difficult and subject to error. The measurement error is in the order of magnitude of the differences in elastic behavior, so it is difficult to analyze further.

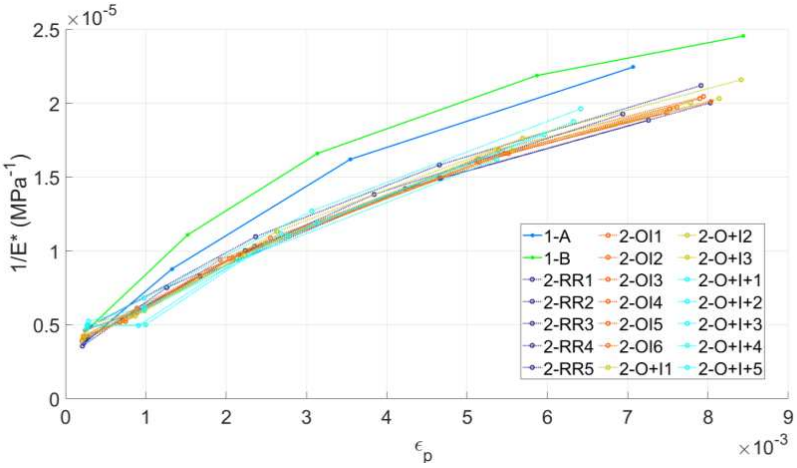

Figure 6. Evolution of at the tangent modulus $1/E^*$ in function of the strain at the beginning of the discharge for the both batches.

In summary, the seal coat layers had limited impact on the slippage and the evolution of the E^* modulus. Indeed, even if they cracked, the thickness of the matrix remained small compared to the core of the material. Their damage was therefore negligible. On the other hand, the changes in the plies composition had an influence on the mechanical behavior. A softer matrix decreased the interfaces slippage but softened the damageable behavior.

4. Conclusion

First, the characteristics of two different batches of tubes were described to investigate the impact of a morphological modification within the plies and the impact of the seal coat layers, respectively. In a second step, the mechanical behavior was analyzed by focusing on the elastic modulus and two characteristic quantities for the matrix cracking part, describing the sliding and the damage progression. Simplified modelling considering the plies as unidirectional composites, allowed relationship with microstructure to be established. Thus, it was highlighted that the seal coat layers allow stiffening and making the composite more isotropic in the elastic part while they have no impact on the behavior in the matrix cracking part. The presence of Si

in the plies makes the matrix in the core more flexible, which results in a decrease of the $E$and E^* moduli, in comparison with reference tubes. A softer matrix also leads to a decrease of the cycle width, which corresponds to the description of the shear-lag model.

For further study, it would be now interesting to describe the cycled behavior in compression. As the cracks perpendicular to the loading direction are closed under compressive loading, it will be possible to obtain additional information on the cracks in shear. These different descriptions would make it possible to evidence the different mechanisms that appear during the matrix-cracking phase of the tubes to describe the damage mechanisms of the composite in more details. This will allow building a damage model representative of the mechanisms based on the shear lag model.

5. References

1. Saucedo-Mora L, Lowe T, Zhao S, Lee PD, Mummery PM, Marrow TJ. In situ observation of mechanical damage within a SiC-SiC ceramic matrix composite. Journal of Nuclear Materials 2016; 481:13-23.
2. Bansal NP, Lamon J. Ceramic matrix composites: materials, modeling and technology. John Wiley & Sons 2014, chapter 13.
3. Terrani KA. Accident tolerant fuel cladding development: Promise, status, and challenges. Journal of Nuclear Materials 2018; 501:13-30.
4. Vagaggini E, Domergue JM, Evans AG. Relationship between hysteresis measurements and the constituent properties of ceramic matric composites: I, theory. Journal of American Ceramic Society 1995; 78:2709-2720.
5. Lissart N, Lamon J. Damage and failure in ceramic matrix minicomposites: experimental study and model. Acta Materialia 1997; 45.3:1025-1044.
6. Lamon J. A micromechanics-based approach to the mechanical behavior of brittle-matrix composites. Composites science and technology 2001; 61.15: 2259-2272.
7. Yun HM, DiCarlo JA, Fox DS. Issues on fabrication and evaluation of SiC/SiC tubes with various fiber architectures. HTCMC-5 2004; NASA/TM-2004-213335.
8. Braun J, Sauder C, Lamon J, Balbaud-Célérier F. Influence of an original manufacturing process on the properties and microstructure of SiC/SiC tubular composites. Composites Part A: Applied Science and Manufacturing 2019; 123:170-179.
9. Sauder C, Lorrette C. Method for producing a composite including a ceramic matrix. U.S. Patent No. 9,145,338. 2015.
10. ISO 20323, Fine ceramics (advanced ceramics, advanced technical ceramics) – Mechanical properties of ceramic composites at ambient temperature in air atmospheric pressure - Determination of tensile properties of tubes, 2018.
11. Michaux A, et al. Young's modulus, thermal expansion coefficient and fracture behavior of selected Si–B–C based carbides in the 20–1200°C temperature range as derived from the behavior of carbon fiber reinforced microcomposites. Journal of the European Ceramic Society 2007; 27.12:3551-3560.
12. Pensée V, Kondo D, Dormieux L. Micromechanical analysis of anisotropic damage in brittle materials. Journal of Engineering Mechanics 2002; 128.8: 889-897.

